International Journal of Applied Pharmaceutics

ISSN- 0975-7058 Vol 16, Issue 4, 2024

Original Article

SYSTEMATIC DEVELOPMENT, OPTIMIZATION AND EVALUATION OF ASCORBIC ACID-COATED SUPER-PARAMAGNETIC IRON OXIDE NANOPARTICLES (SPIONS)

SAMEEA AHMED KHAN*, RAJESH SHARMA

Devi Ahilya Vishwavidyalaya, Takshashila Campus, Khandwa Road (Ring Road), Indore-452001, Madhya Pradesh, India
***Corresponding author: Sameea Ahmed Khan; *Email: sameeak63@gmail.com**

Received: 18 Apr 2024, Revised and Accepted: 25 May 2024

ABSTRACT

Objective: In this study, Ascorbic acid-coated Super-Paramagnetic Iron Oxide Nanoparticles (AA-SPIONs) were synthesized, optimized, and further evaluated.

Methods: The nanoparticles were synthesized using the co-precipitation method, optimized by Box-Behnken Design (Design Expert® software). The formulation was then characterized for several *in vitro* attributes such as particle size distribution, zeta potential, Fourier Transform Infrared Spectroscopy (FTIR), X-ray diffraction (XRD), Differential Scanning Calorimetry (DSC), and Vibration Sample Magnetometry (VSM).

Results: An optimized formulation was designed and synthesized. It showed an average size of ~260 nm with 24 mV zeta potential. The small size and electrostatic stability suggested an even distribution of particles in the bloodstream. FTIR revealed the interaction of AA with iron oxide. XRD studies and DSC thermograms ascertained the crystallinity of the iron formulation complying that the particles behaved as a single-domain magnetic crystal. The glass transition temperature of the coated nanoparticles was found to be 135.463ºC. Vibration sample magnetometry displayed the saturation magnetization value to be 2.87 emu g^{-1}, which indicated the retained super-paramagnetic nature of the nanoparticles.

Conclusion: The results were in concordance with the aim of this research work.

Keywords: Magnetic nanoparticles, SPIONs, Box-behnken design, Metal nanoparticles

DOI: https://dx.doi.org/10.22159/ijap.2024v16i4.51168 Journal homepage: https://innovareacademics.in/journals/index.php/ijap

INTRODUCTION

Iron-deficiency anemia is a condition in which the blood lacks healthy Red Blood Cells (RBCs) due to insufficient iron in the body [1]. It is characterized by symptoms such as extreme fatigue, pale skin, weakness, shortness of breath, dizziness, etc. [2, 3] This deficiency is prevalent in menstruating women, children, and elderly people [4]. Oral route medication is the first-line treatment for anemia because it is cost-effective, easy to obtain, and offers better patient compliance but it poses problems like gastric disturbances (constipation, diarrhea, abdominal pain, etc.), heavy uterine bleeding, bowel diseases, etc [5-7]. On the other hand, *iv* iron sometimes leads to a major Serious Adverse Event (SAE) of anaphylaxis that can be dangerous [8, 9].

Focusing on the delivery system, Super-Paramagnetic Iron Oxide Nanoparticles (SPIONs) have captured interest due to their magnetic nature, ability to resist changes in magnetic field (coercivity), large surface-to-volume ratio, non-toxicity, and low Curie temperature [10]. The types of iron core include Magnetite (Fe_3O_4), Haematite (alpha-Fe_2O_3) or Anti-ferromagnetic, Maghemite (gamma-Fe_2O_3) or Ferrimagnetic [11]. SPIONs can be synthesized through various methods, including mechano-chemical (i. e., electrodeposition, laser ablation arc discharge, combustion, and pyrolysis) and chemical (reverse micelle, template-assisted synthesis, sol-gel synthesis, hydrothermal, co-precipitation, etc.) methods [12, 13]. Due to their nano-size, prolonged release is possible, leading to lower doses and better absorption. The safety, biocompatibility, and surface modification make them a suitable candidate for applications as therapeutics, diagnostics, and theranostics as well [14].

Response surface methodology (RSM) is utilized in drug dosage form development to optimize the process parameters. When designing experiments, the response surface approach is frequently employed to reduce the number of trials for a given number of parameters and their values. It is superior to other design methods in many ways [15, 16]. According to the experimental design, experiments are carried out, and results, including output, are reported. To determine the variables that significantly affect the response, analysis of variance (ANOVA) is utilized [17]. In order to acquire an outcome function, process parameters are optimized and regression equations are built to predict the response. For the RSM evolved, 2D and 3D graphs were produced using the "Design-expert" software. These graphs clearly show which process variable is dominant over the others and in what order, and they also show the trend of how the variables interact during the process [18].

The novelty behind this dosage form development was to use the iron nanoparticle core itself to treat IDA. The formulation uses both forms of iron. The+2 and+3 states of Ferrous sulphate heptahydrate and Ferric chloride anhydrous respectively; thereby increasing the level of iron in the body [19]. The nanoparticles were synthesized via the co-precipitation method. We have chosen the oral route as it is the first-line treatment and promises better patient compliance, affordability, and most importantly, eliminating the risk of anaphylaxis [20, 21]. In addition to this, it will lead to a lowering of doses and prolong the circulation time along with being safe and biocompatible with the gastrointestinal (GI) environment, unlike the aforementioned iron salts [22, 23]. The study aims to design, optimize, and characterize coated iron nanoparticles. The critical formulation attributes and process parameters were identified by preliminary trials, followed by their systematic optimization using the Response Surface Methodology (RSM) tool of Quality by Design (QbD). Box-Behnken design (BBD) demonstrated the effect of independent variables (i.e. AA and sorbitol concentration, sonication time) on the dependent ones (i.e., particle size (PS), polydispersity index (PDI), and zeta potential). The developed SPIONs were characterized for different *in vitro* attributes [24].

MATERIALS AND METHODS

Ferrous sulphate heptahydrate ($FeSO_4.7H_2O$) and Ferric chloride anhydrous ($FeCl_3$) were purchased from loba Chemie Pvt. ltd., Mumbai, India. AA was brought from SRL Research lab Pvt. ltd., Mumbai and D-Sorbitol was purchased from Thomas Baker Pvt. ltd., Mumbai, India, and used as received. Ammonia solution (25% v/v AR) was purchased from S D Fine-Chem. ltd., Mumbai, India. HPLC water was purchased from loba Chemie Pvt. ltd., Mumbai, India. All chemicals were of analytical grade and were used without further purification.

Formulation development synthesis of blank SPIONs

Co-precipitation method was used to synthesize an aqueous dispersion of blank SPIONs. 10 ml of 25% solution of conc. ammonia was added dropwise in the reaction flask containing solutions of Ferrous Sulphate Heptahydrate and Ferric Chloride (anhydrous) in HPLC water (2:1 molar ratio). The mixture was continuously stirred at 1600-2000 rpm and temperature was maintained at 60-65°C. The reaction was carried under an inert atmosphere of nitrogen in the flask for an hour for the complete aging of all iron salts. A black coloured solution was formed at the end of the experiment, indicating the formation of blank SPIONs or uncoated SPIONs. The blank SPIONs and supernatant liquid were separated by a magnetic decantation process. The blank SPIONs were washed three times with nitrogen-purged HPLC water and centrifuged at 14,500 rpm for 30 minutes at 4°C (High-Speed Refrigerated Micro Centrifuge; MX-305; Tomy, Japan). It was then washed and reconstituted in 10 ml of nitrogen-purged HPLC water. Blank SPIONs were lyophilized in the lyophilizer (Triad TM, labconco, MO) using 5% mannitol as lyoprotectant and were stored in airtight amber-colored containers at 4°C for further use [25].

$$Fe^{2+} + 2Fe^{3+} + 8OH^- \xrightarrow{\text{alkaline pH}\sim10,65^{\circ}C} Fe_3O_4 + 4H_2O$$

Synthesis of ascorbic acid coated SPIONs (AA-SPIONs)

AA-coated SPIONs were prepared using a similar procedure as mentioned in section 3.1 except that the AA in sorbitol solution was incorporated into the reaction 30 minutes before the addition of liquid ammonia. Ferrous Sulphate Heptahydrate, Ferric Chloride (anhydrous), AA in sorbitol and liquid ammonia were added in the respective order, continuously stirred and visually examined for the formation of a suitable and re-constitutable dispersion. It was found that the ferrofluid was easily re-dispersible upon shaking. AA-SPIONs were washed three times with nitrogen-purged HPLC water and centrifuged at 14,500 rpm for 30 minutes at 4 °C (High-Speed Refrigerated Micro Centrifuge; MX-305; Tomy, Japan). It was then washed and reconstituted in 10 ml of nitrogen-purged HPLC water. The procedure was then followed for optimization. AA-SPIONs were lyophilized in the lyophilizer (Triad TM, labconco, MO) using 5% mannitol as lyoprotectant and were stored in air-tight amber-colored containers at 4 ºC for further use.

Formulation optimization

On the basis of initial screening experiments, AA concentration, sorbitol concentration and sonication time were considered as the factors that critically influence the values of PS, PDI and zeta potential. Using response surface methodology (RSM), the experimental data was fitted to a model for optimizing the process. In this work, Box-Behnken Design (BBD) was used to assess the relationships between independent variables and their dependent responses by performing 17 experiments containing 12 factorial points and 5 replicates of the central point by defining 3 independent variables at 3 levels: low (-1), medium (0) and high (1). Design Expert software (v. 11.1.2.0, Stat-Ease Inc., Minneapolis, MN) was used for formulation optimization and statistical analysis of data. Table 1 describes the upper, mid and lower limit values of AA, sorbitol and sonication time in coded values such as-1, 0 and 1, respectively. Using BBD, a second-order polynomial function model was employed for the optimization of the manufacturing process:

$$Y = \beta0+\beta1A+\beta2B+\beta3C+\beta11A^2+\beta22B^2+\beta33C^2+\beta12AB+\beta13AC+\beta23BC \quad (1)$$

where Y is the predicted response, β_1, β_2 and β_3 are the linear coefficients, β_{11}, β_{22} and β_{33} are the squared coefficients and β_{12}, β_{13} and β_{23} are the interaction coefficients, β_0 is the intercept of the equation, and A, B and C are the independent variables. 3D response surface plots are shown to provide a clear understanding the relation between the independent variables and the dependent responses. We have optimized the condition for a minimum value of PS, PDI and an optimum value of zeta potential. Finally, the optimized formulation (suggested by software) with the predicted values of the responses were compared with experimental values to evaluate the prognostic ability and desirability of the model used in RSM.

Table 1: Specification of the minimum, middle and maximum quantity of the three independent variables

Factor		Levels		
		Level 1 (-1)	Level 2 (0)	Level 3 (1)
Independent variables				
A.	Ascorbic acid (mg)	10	55	100
B.	Sorbitol (mg)	50	115	180
C.	Sonication time (min)	1	3	5
Dependent variables				
Y1 Particle size (nm); Y2 Poly dispersity index; Y3 Zeta potential (mV)				

Characterization of SPIONs particle size and zeta potential measurement

Particle size and polydispersity index of the nanoparticles were analyzed using Malvern Zetasizer (Nano-ZS, Malvern, UK). The samples were diluted with HPLC water and ultra-sonicated for 3 min at room temperature. Sonication was done at a detection angle of 90° and 120W power (Branson 8210, Branson Ultrasonics Co., Danbury, CT, USA). The measurements were conducted in triplicate. For zeta potential measurement, the diluted samples were placed in a folded capillary cell and measured using Zetasizer [26, 27].

Fourier transform-infrared spectroscopy (FT-IR)

FTIR spectroscopic analysis of the formulation was carried out using the Potassium Bromide (KBr) pellet technique. An accurately weighed quantity of lyophilized blank SPIONs and AA-SPIONs (5 mg) were mixed with KBr (1:1) and later converted into pellets using a hydraulic press. The scanning range was taken to be 4000-400 cm^{-1} and TENSORTM 37, Bruker was used [28].

X-ray diffraction (XRD)

An X-ray beam was made to fall at different angles on the lyophilized samples and the diffraction intensity was recorded as a function of incident angle by X-ray diffractometer (Ultima IV), using monochromatic Ni-filtered Cu–K radiation, a voltage of 40 kV, a current of 30 mA radiation. Patterns were obtained by using a step width of 0.04º with a detector resolution of 2ɵ (diffraction angle) between 10º and 80º at ambient temperature [29].

Differential scanning calorimetry (DSC)

The lyophilized samples of blank SPIONs and AA-SPIONs (about 5 mg) were loaded and sealed into an aluminum pan with a DSC loading puncher. The sample holder temperature range was kept at 50-300 °C at a heating rate of 10 °C/min, under a nitrogen atmosphere. The calorimeter used was Perkin Elmer Pyris 6 DSC (Massachusetts, U. S. A). Transition temperature analysis was studied by DSC (Perkin Elmer, USA).

Vibrating sample magnetometry (VSM)

Vibrating sample magnetometry (VSM) (LDJ9600-1, lDJ, USA) was used to investigate the magnetic properties of pristine magnetite and AA-SPIONs in the form of magnetization curves. The lyophilized samples were mounted on a sample holder and a magnetic field was applied in the range of 0-18 kOe for this study. Micro Sense Easy VSM software was used for data acquisition and processing [30].

RESULTS AND DISCUSSION

Formulation design

SPIONs were synthesized using the co-precipitation method as it is the most convenient and cost-effective method is co-precipitation method

which is simple, reliable, and can be easily followed in the laboratory. In this method, both the iron salts i. e., ferrous and ferric salts are mixed in a ratio of 2:1 in a basic environment to avoid oxidation. The reaction takes place at room temperature or elevated temperature. This method critically affects the physical structure, morphology, and chemical properties of the nanosized iron oxide particles [31, 32].

Fig. 1: (a) AA-coated SPIONs (final formulation) (b) lyophilized AA-SPIONs

Formulation optimization using box-behnken design (BBD)

The three independent variables chosen were AA concentration, sorbitol concentration, and sonication time, while particle size (PS), polydispersity index (PDI) and zeta potential were selected as the responses. The values of responses R1 (PS), R2 (PDI) and R3 (Zeta potential) ranged from 297.6 to 922.6 nm, 0.21 to 0.751 and-26.3 to 6.1mV (table 2). Ratios of maximum to minimum response for PS, PDI and Zeta potential were 3.1, 3.57 and-0.23, respectively. Power transformation was not required for all three values as the ratio was less than 10. Model source was selected by analyzing all three responses based on the sequential model sum of squares, lack of fit and model summary statistics. The p-value (<0.0001), low SD (standard deviation), and predicted residual error sum of square (PRESS) value suggested selecting a quadratic model for all responses. ANOVA (Analysis of Variance) identifies the significant factors that affect the responses. The "Predicted R-Squared'' value of 0.8827, 0.8643 and 0.8514 was in agreement with the "Adjusted R-Squared'' value of 0.9832, 0.9806 and 0.9788 of R1, R2 and R3 respectively. The difference between predicted R-squared values and adjusted R-squared values was found to be less than 0.2 for all three responses. The Model F values for responses R1, R2 and R3 were 105.28, 90.92 and 82.94. This data confirmed that the model was significant. Using BBD, a second-order polynomial function model was applied for the optimization of the response variables R1, R2 and R3. The equations with variables A, B, and C being assigned to the independent factors could be used to make predictions about response for given levels of each factor. These equations were useful in identifying the relative impact of these factors by comparing the factor coefficients. The high levels of the factors were coded as+1 and the low levels were coded-1.

Table 2: Box-behnken experimental design displaying 17 runs and their corresponding responses

Run	Factor 1	Factor 2	Factor 3	Response 1	Response 2	Response 3
	A: Ascorbic acid	B: Sorbitol	C: Sonication time (ST)	R1: Particle size (PS)	R2: Polydispersity index (PDI)	R3: Zeta potential
	mg	mg	Minutes	nm		mV
1	55	115	3	297.6	0.357	-25.8
2	55	180	5	864.4	0.495	6.1
3	10	115	1	575.3	0.54	-20.7
4	100	50	3	740.6	0.54	-23.3
5	10	115	5	888.2	0.53	3.71
6	100	115	1	570.3	0.407	-26.3
7	55	115	3	297.6	0.357	-25.8
8	55	115	3	297.6	0.357	-25.8
9	55	50	1	447.1	0.32	-18.2
10	55	115	3	297.6	0.357	-25.8
11	55	115	3	297.6	0.357	-25.8
12	55	50	5	816.2	0.223	-7.32
13	55	180	1	380.4	0.334	-12.9
14	100	115	5	922.6	0.517	-12.7
15	100	180	3	580.4	0.21	-13.5
16	10	180	3	679.4	0.751	-8.18
17	10	50	3	650.2	0.24	-13.6

Particle size= $297.60+2.60*A - 18.69*B+189.79*C - 47.35*AB+9.85*AC+28.72*BC+238.56* A^2+126.49* B^2+202.94* C^2$

PDI= $0.357 - 0.0484*A+0.0584*B+0.0205*C - 0.2103*AB+0.0300*AC+0.0645*BC+0.1169* A^2-0.0386* B^2-0.0246* C^2$

Zeta potential= $-25.8 - 4.63*A+4.24*B+8.49*C+1.10*AB - 2.70*AC+2.03*BC+2.62* A^2+8.54* B^2+9.18* C^2$

In the equations described, A, B, and C refer to the AA concentration, sorbitol concentration and sonication time, respectively. The negative coefficients of A in PDI and zeta potential indicate that there is a decrease in PDI and zeta potential when AA concentration is increased. Negative coefficients of B in particle size indicate that there is a decrease in particle size when sorbitol concentration is increased. For positive coefficients of C, it indicates that increasing sonication time leads to increased particle size, PDI, and zeta potential.

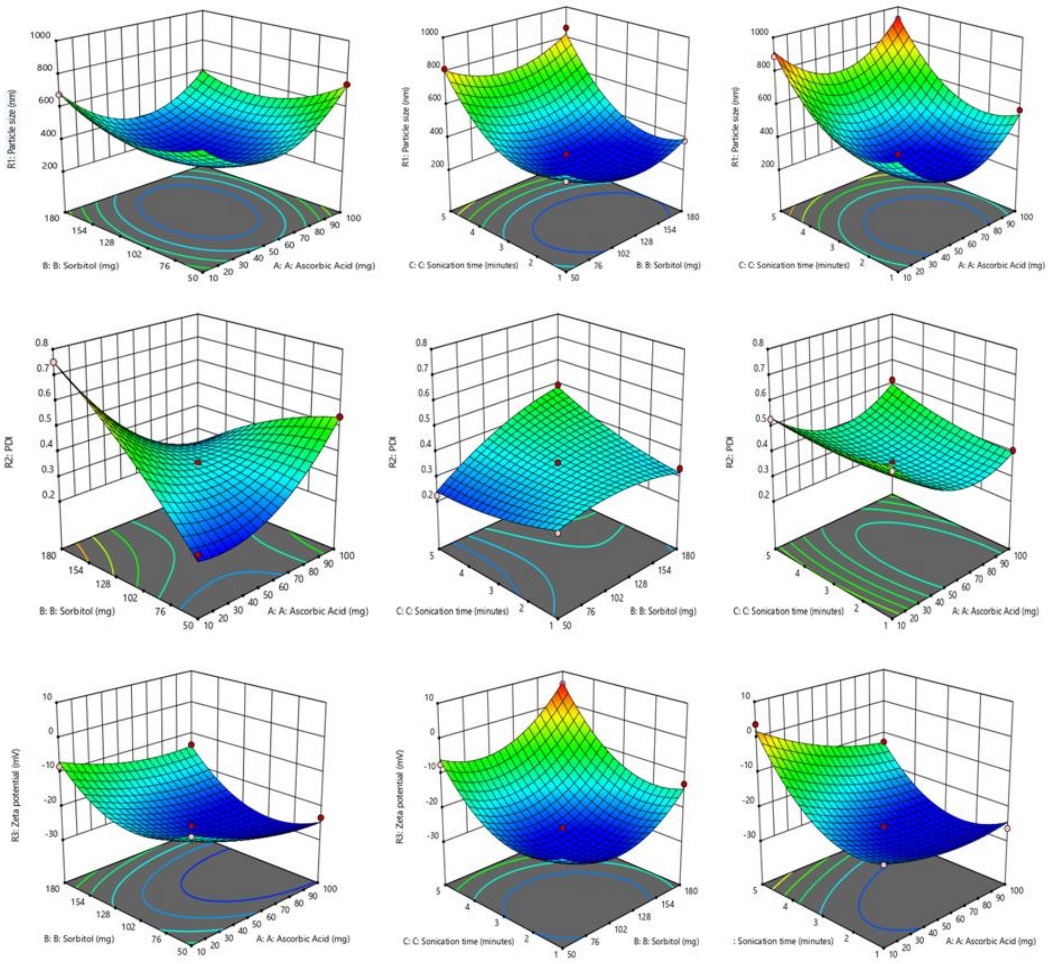

Fig. 2: Response surface plots for particle size, PDI, and sonication time

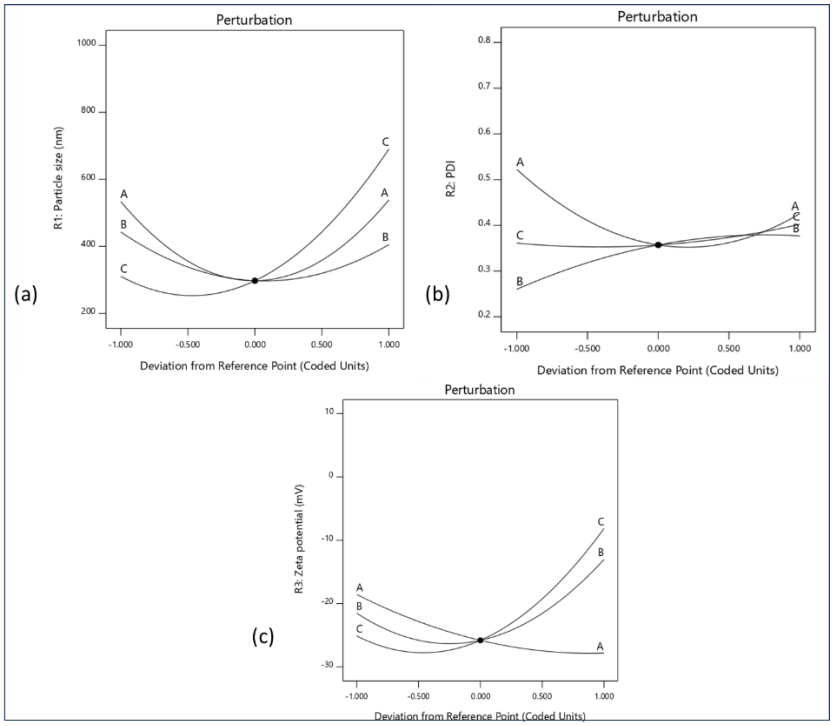

Fig. 3: Perturbation plots to see the sensitivity of factors A, B, and C on (a) PS (b) PDI (c) Zeta potential

Effect of independent variables on responses

Fig. 2 shows the response surface plots for PS, PDI and zeta potential, respectively. These plots are depicted in 3-D space for better understanding. Both below and above 55 mg concentration of AA, particle size was higher. At low concentrations (<55 mg AA), the coating agent was not able to cap whole of iron oxide cores, causing aggregation and so, an increase in PS. However, at a concentration>55 mg AA, extra AA was present in the resultant mixture causing the coating of the iron oxide core and further forming clusters. At constant AA concentration, both below and above 100 mg Sorbitol, particle size was higher. This similar phenomenon can be attributed to Sorbitol being a sub-component of the coating solution. As the sonication time is increased at constant AA concentration, PS decreases. Higher sonication time provided energy for reducing the size of the particles. However, excessive conditions led to the aggregation of these broken particles. An increase in particle size reinforced an increase in PDI and vice versa. There was an inverse relationship between AA and sorbitol concentration upon zeta potential. However, no major impact was derived from it. Also, it was noted that upon increasing the sonication time, zeta potential increased. This could be due to shear force overpowering interfacial force (i. e., force that holds the particles together).

Optimal formulation was decided with a precise criterion on minimizing PS, PDI and zeta potential. Employing numerical optimization of experimental design, AA concentration 50 mg, Sorbitol 90 mg and sonication time 3 min was taken as the final formulation. Table 3 shows the validation table recording responses of predicted and observed values of various parameters.

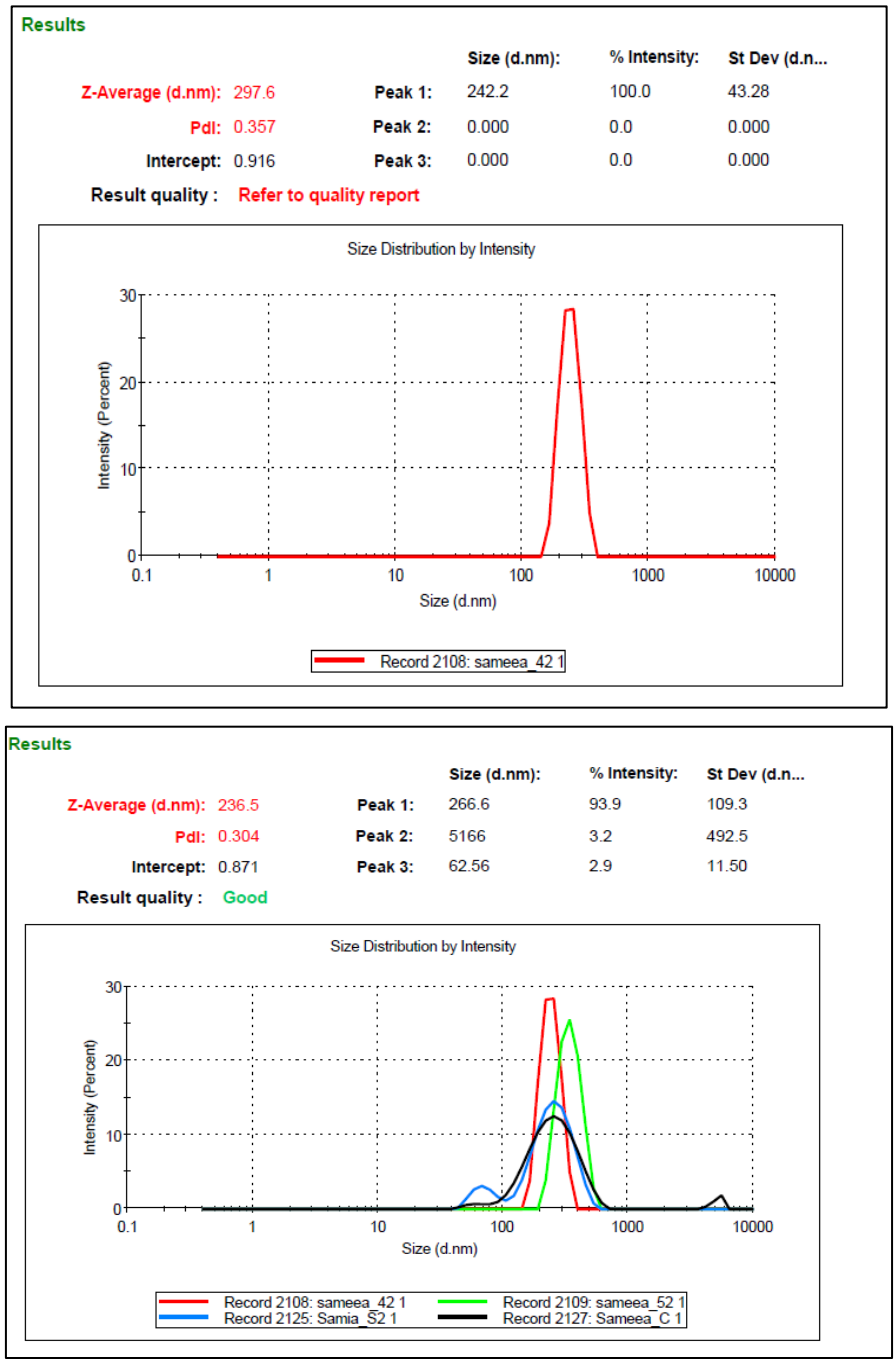

Fig. 4: Particle size distribution of the AA-SPIONs

Table 3: Validation of optimized values for formulation parameter of AA-SPIONs, SPIONs: Super-paramagnetic iron oxide nanoparticles; PDI: Polydispersity index

Formulation	Composition			Response		
	Ascorbic acid (mg)	Sorbitol (mg)	Sonication time (min)	Particle size (nm)	PDI	Zeta potential (mV)
SPIONs (Predicted)	48.4	79.7	2.3	311.9	0.315	-26.3
SPIONs (Observed)	50	90	3	264±39.22*	0.374± 0.015*	-24.37±3.2*

*Data represented as mean±SD n=3

Characterization of optimized formulation

Particle size distribution and zeta potential

The particle size of the developed formulation was found to be in the range of 200-400 nm. As shown in fig. 4, the AA-SPIONs exhibited a particle size of 264±39.22 nm with a PDI of 0.374±0.015. The small size suggested that the formulation would be evenly distributed into the bloodstream without forming clusters. low PDI value depicted the homogeneity of particle sizes in the formulation. The results pointed towards a narrower size distribution and uniform particle size. The zeta potential was found to be-24.37±3.2 mV as seen in fig. 5, and thus lay in the range of-30 mV to+30 mV. This showed that the particles were electrostatically stable. This zeta potential value indicated good colloidal stability by the electrostatic repulsive inter-particle interaction. The negative value of zeta potential was due to the presence of carbonyl and hydroxyl groups of AA and sorbitol, which constituted the coating of SPIONs.

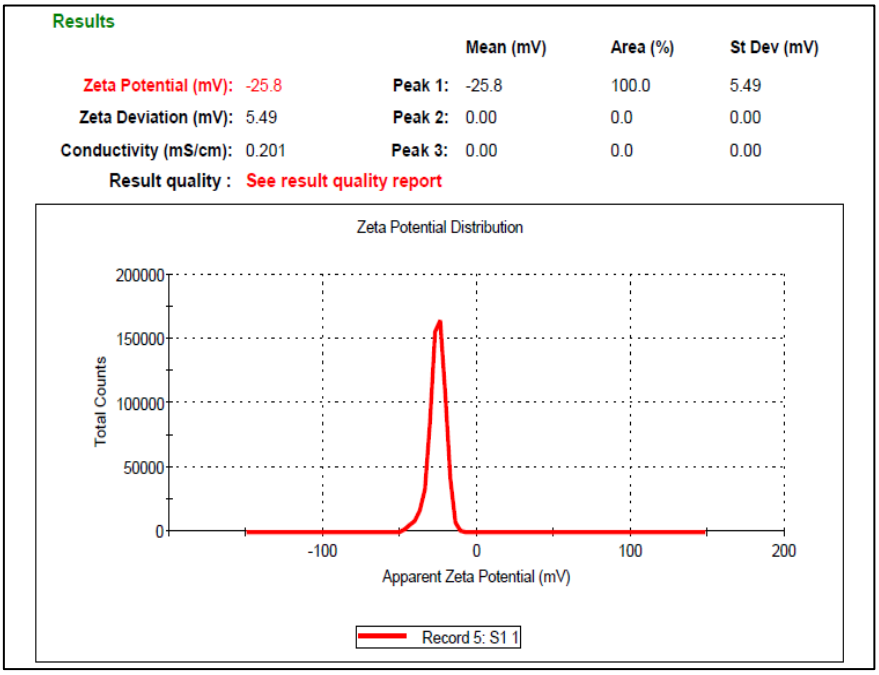

Fig. 5: Zeta potential graph of the AA-SPIONs

FTIR analysis

The pellets were scanned between 4000 to 400 cm^{-1} to get the characteristic spectra as shown in fig. 6. The FT-IR spectrum of SPIONs showed the band at 1399 cm^{-1}. The sharp peak at 1625 cm^{-1} is ascribed to bending H^+ and OH^-vibrations. The characteristic absorption peak of tetrahedral Fe–O–Fewas identified at 660 cm^{-1} for SPIONs. In AA-SPIONs, the acidic functional group-COOH-became–COO-to attach to the surface of iron oxide. This modification was known as chemical adsorption. It was known that the absorption peak of 1750 cm^{-1} is characteristic of the presence of AA because of the stretching vibration of C=O present in the five-membered lactone ring. In the AA-SPIONs spectra, the band disappeared, indicating covalent bonding of the biomolecule on the surface. The bands at 1674 cm^{-1} and 1420 cm^{-1} could be attributed to the asymmetric and symmetric-COO-stretches. Due to the presence of AA, the stretching vibration of the C-C double bond and the peak of enol-hydroxyl were noted at 1648 cm-1 and 1322 cm^{-1}, respectively. Therefore, it could be derived that AA was effectively capped onto the surface of iron oxide NPs [33, 34].

X-ray diffraction (XRD)

In order to identify the physical state and crystallinity, XRD spectra of Fe_3O_4 and XRD of the formulation were carried out. The XRD pattern of pristine magnetite is shown in fig. 7. The characteristic crystalline peaks at various 2θ positions of 10°, 13°, 17°, 21°, 26°, 30.5°, 33°, 39°, 43.4°, 50°, 53.8°, 57.4°, 64°, 66° and 70° corresponding to *hkl* values of {130}, {152}, {166}, {181}, {149},{220}, {311}, {183}, {400}, {164}, {422}, {146}, {160},{155} and {154}. The crystallographic structure along with its composition and physical characteristics of the compound can be obtained. Bragg's reflection showed a good correspondence with standard magnetite (Fe_3O_4) XRD patterns, which depict that Fe_3O_4 NPs have a cubic spinel structure. XRD analysis of AA-SPIONs showed similar peaks, which proved that there was no major change in the crystallinity of the nanoformulation. As a commonly known fact, Ascorbic acid itself possesses crystalline properties; hence the coating did not result in a phase change of bare Fe_3O_4. This confirmed that the coating took place efficiently without disrupting the pattern of the arrangement of constituent particles [35].

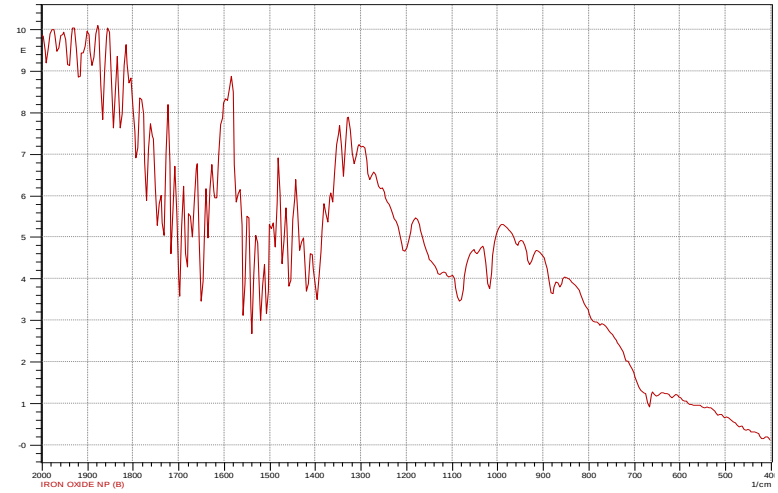

(a)

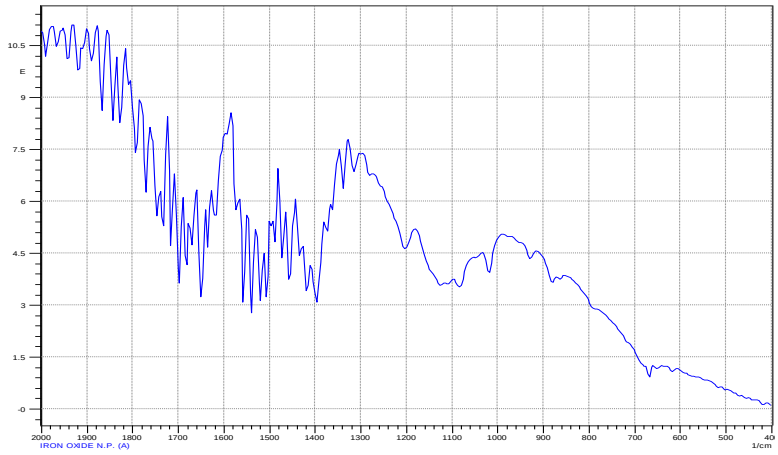

(b)

Fig. 6: FTIR of (a) Blank SPIONs (b) AA-SPIONs

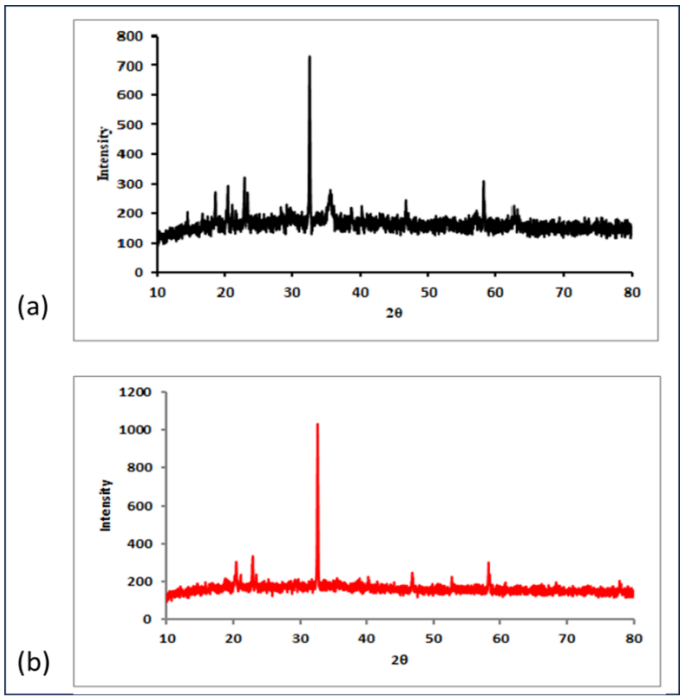

Fig. 7: XRD of (a) Blank SPIONs (b) AA-SPIONs

Differential scanning calorimetry (DSC)

Transition temperature analysis was studied by DSC (Perkin Elmer, USA). As seen in fig. 8, the peak was observed at 138.289 °C for blank SPIONs (A) and 135.463ºC for AA-SPIONs (B), indicating that there was no change in the crystallinity of the structure. These peaks lay around 130 °C which showed that an exothermic reaction took place upon heating due to crystallization. This data also indicated a high degree of purity of the samples and the absence of interfering impurities. AA and iron oxide nanoparticles are crystalline in nature and their interaction in the graph of AA-SPIONs indicated that there was no change in the crystallinity of the structure [36].

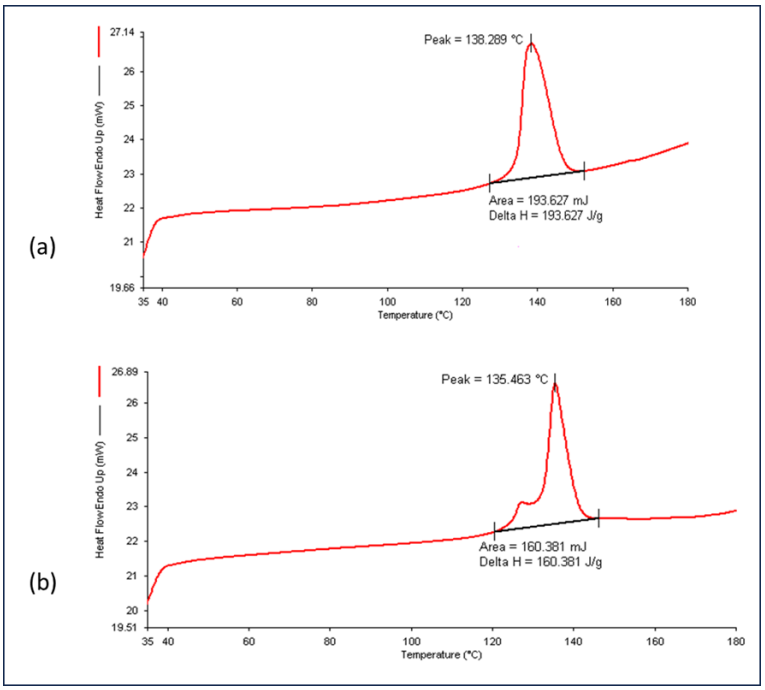

Fig. 8: DSC thermograms of (a) Blank SPIONs (b) AA-SPIONs

Vibrating sample magnetometry (VSM)

The magnetic properties of pristine magnetite and AA-SPIONs were confirmed by vibrating sample magnetometry (VSM). A magnetization versus magnetic field (M–H loop) curve was plotted at room temperature, as illustrated in fig. 9. In the hysteresis M-H curves, the presence of almost super-imposable upward and downward segments proves that the formulations are superparamagnetic with very small magnetic cores. There was a major difference observed in the value of saturation magnetization (Ms) for blank SPIONs (9.05 emu g^{-1}) as compared to AA-SPIONs (2.87 emu g^{-1}) after drug coating. This might be due to the presence of non-magnetic component AA on the surface of SPIONs, which contributed to a decrease in the overall super-paramagnetic iron oxide content [37-39].

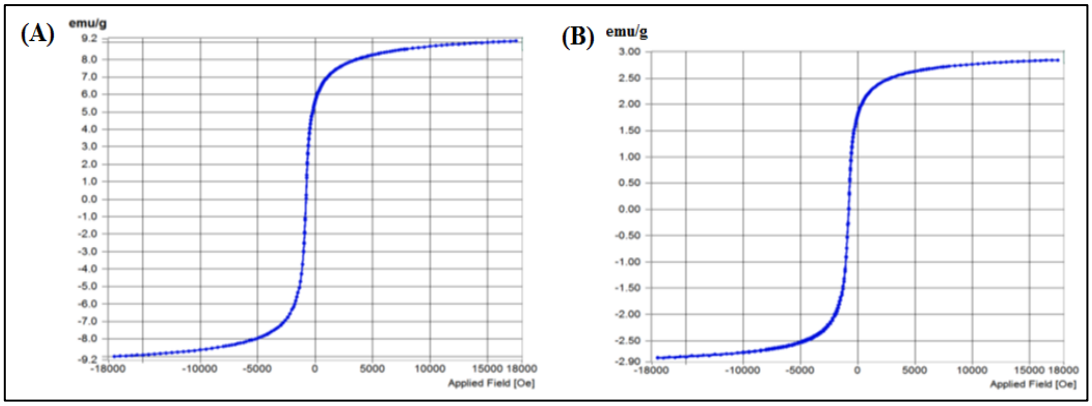

Fig. 9: Vibration sample magnetometry data showing the M–H curves for (a) Blank SPIONs (b) AA-SPIONs

CONCLUSION

This study exhibits the development of an effective and stable Ascorbic acid-coated superparamagnetic iron oxide nanoparticles (AA-SPIONs) using a facile, one-pot synthesis via co-precipitation method. Using BBD, an optimized colloidally stable (zeta potential,-24.37±3.2 mV), nanometric (particle size, 264±39.22 nm), and super-paramagnetic formulation with iron oxide core and AA coating was obtained. Characterization studies were also performed that revealed distinctive properties of the iron oxide nanoparticles. FTIR revealed characteristic peaks of standard iron nanoparticles and also confirmed the interaction of iron oxide with AA. The transition temperature of AA-SPIONs was found to be 135.463 °C.

The VSM data presented the value of saturation magnetization (Ms) for AA-SPIONs to be 2.87 emu g^{-1}. In conclusion, the developed formulation with synergistic effects of being nano-particulate, decreased dose, and no toxic effects was found to be a good replacement for conventional iron formulations. Iron oxide nanoparticles encompass an extensive range of uses and have become the cynosure of every researcher's eye.

ACKNOWLEDGEMENT

All authors have contributed to this work. Sameea: Studying, experimenting and drafting; Prof. Rajesh: Review, editing and supervision.

FUNDING

There was no source of funding for this work.

AUTHORS CONTRIBUTIONS

All authors have contributed equally

CONFLICT OF INTERESTS

There is no conflict of interest between the authors. The authors have no other relevant affiliations or financial involvement with any organization or entity with a financial interest in or financial conflict with the subject matter or materials discussed in the manuscript apart from those disclosed.

REFERENCES

1. De Franceschi L, Iolascon A, Taher A, Cappellini MD. Clinical management of iron deficiency anemia in adults: systemic review on advances in diagnosis and treatment. Eur J Intern Med. 2017;42:16-23. doi: 10.1016/j.ejim.2017.04.018, PMID 28528999.
2. Tettamanti M, lucca U, Gandini F, Recchia A, Mosconi P, Apolone G. Prevalence, incidence and types of mild anemia in the elderly: the "Health and anemia" population-based study. Haematologica. 2010;95(11):1849-56. doi: 10.3324/haematol.2010.023101, PMID 20534701.
3. Ganz T. Hepcidin–a regulator of intestinal iron absorption and iron recycling by macrophages. Best Pract Res Clin Haematol. 2005;18(2):171-82. doi: 10.1016/j.beha.2004.08.020, PMID 15737883.
4. Killip S, Bennett JM, Chambers MD. Iron deficiency anemia. Am Fam Physician. 2007;75(5):671-8. PMID 17375513.
5. Peyrin Biroulet L, Williet N, Cacoub P. Guidelines on the diagnosis and treatment of iron deficiency across indications: a systematic review. Am J Clin Nutr. 2015;102(6):1585-94. doi: 10.3945/AJCN.114.103366, PMID 26561626.
6. Gour N, Chawla S. Prevalence of anemia among patients with cancer: a complex phenomenon. Cancer Res Stat Treat. 2021;4(1):166. doi: 10.4103/crst.crst_18_21.
7. Kassebaum NJ, Jasrasaria R, Naghavi M, Wulf SK, Johns N, lozano R. A systematic analysis of global anemia burden from 1990 to 2010. Blood. 2014;123(5):615-24. doi: 10.1182/BLOOD-2013-06-508325, PMID 24297872.
8. Bharati S, Pal M, Sen S, Bharati P. Malnutrition and anaemia among adult women in India. J Biosoc Sci. 2019;51(5):658-68. doi: 10.1017/S002193201800041X, PMID 30929649.
9. Bharati S, Pal M, Bharati P. Prevalence of anaemia among 6- to 59 mo old children in India: the latest picture through the NFHS-4. J Biosoc Sci. 2020;52(1):97-107. doi: 10.1017/S0021932019000294, PMID 31104639.
10. Arruebo M, Fernandez Pacheco R, Ibarra MR, Santamaria J. Magnetic nanoparticles for drug delivery. Nano Today. 2007;2(3):22-32. doi: 10.1016/S1748-0132(07)70084-1.
11. El-Boubbou K. Magnetic iron oxide nanoparticles as drug carriers: preparation, conjugation and delivery. Nanomedicine (Lond). 2018;13(8):929-52. doi: 10.2217/NNM-2017-0320, PMID 29546817.
12. Inozemtseva OA, German SV, Navolokin NA, Bucharskaya AB, Maslyakova GN, Gorin DA. Encapsulated magnetite nanoparticles: preparation and application as a multifunctional tool for drug delivery systems. Nanotechnol Biosens. 2018. p. 175-92. doi: 10.1016/B978-0-12-813855-7.00006-4.
13. Wu W, Jiang CZ, Roy VA. Designed synthesis and surface engineering strategies of magnetic iron oxide nanoparticles for biomedical applications. Nanoscale. 2016;8(47):19421-74. doi: 10.1039/C6NR07542H, PMID 27812592.
14. Laurent S, Saei AA, Behzadi S, Panahifar A, Mahmoudi M. Superparamagnetic iron oxide nanoparticles for delivery of therapeutic agents: opportunities and challenges. Expert Opin Drug Deliv. 2014;11(9):1449-70. doi: 10.1517/17425247.2014.924501, PMID 24870351.
15. Arpna I, Ahmed Masheer KA. Box-behnken design for optimization of formulation variables for controlled release gastroretentive tablet of verapamil hydrochloride. Int J App Pharm. 2023;15(1):256-63. doi: 10.22159/ijap.2023v15i1.46489.
16. Patel M, Khan MA. Optimization, development and evaluation of repaglinide controlled release gastro-retentive floating tablet using central composite design. Int J App Pharm. 2023;15(1):218-26. doi: 10.22159/ijap.2023v15i1.46493.
17. Janko C, Zaloga J, Pottler M, Durr S, Eberbeck D, Tietze R. Strategies to optimize the biocompatibility of iron oxide nanoparticles- "SPIONs safe by design". J Magn Magn Mater. 2017;431:281-4. doi: 10.1016/j.jmmm.2016.09.034.
18. Beg S, Rahman M, Kohli K. Quality-by-design approach as a systematic tool for the development of nanopharmaceutical products. Drug Discov Today. 2019;24(3):717-25. doi: 10.1016/j.drudis.2018.12.002, PMID 30557651.
19. Du J, Cullen JJ, Buettner GR. Ascorbic acid: chemistry, biology and the treatment of cancer. Biochim Biophys Acta. 2012;1826(2):443-57. doi: 10.1016/j.bbcan.2012.06.003, PMID 22728050.
20. Mccurdy PR. Parenteral iron therapy-a new iron-sorbitol citric acid complex for intramuscular injection. Ann Intern Med. 1964;61:1053-64. doi: 10.7326/0003-4819-61-6-1053, PMID 14233826.
21. Mansouri M, Nazarpak MH, Solouk A, Akbari S, Hasani Sadrabadi MM. Magnetic responsive of paclitaxel delivery system based on SPION and palmitoyl chitosan. J Magn Magn Mater. 2017;421:316-25. doi: 10.1016/j.jmmm.2016.07.066.
22. Mallick N, Anwar M, Asfer M, Mehdi SH, Rizvi MM, Panda AK. Chondroitin sulfate-capped super-paramagnetic iron oxide nanoparticles as potential carriers of doxorubicin hydrochloride. Carbohydr Polym. 2016;151:546-56. doi: 10.1016/j.carbpol.2016.05.102, PMID 27474599.
23. Mohapatra S, Asfer M, Anwar M, Ahmed S, Ahmad FJ, Siddiqui AA. Carboxymethyl Assam Bora rice starch coated SPIONs: synthesis, characterization and *in vitro* localization in a microcapillary for simulating a targeted drug delivery system. Int J Biol Macromol. 2018;115:920-32. doi: 10.1016/j.ijbiomac.2018.04.152, PMID 29723619.
24. Anwar M, Asfer M, Prajapati AP, Mohapatra S, Akhter S, Ali A. Synthesis and *in vitro* localization study of curcumin-loaded SPIONs in a microcapillary for simulating a targeted drug delivery system. Int J Pharm. 2014;468(1-2):158-64. doi: 10.1016/j.ijpharm.2014.04.038, PMID 24746694.
25. Gupta AK, Gupta M. Synthesis and surface engineering of iron oxide nanoparticles for biomedical applications. Biomaterials. 2005;26(18):3995-4021. doi: 10.1016/j.biomaterials.2004.10.012, PMID 15626447.
26. Laurent S, Forge D, Port M, Roch A, Robic C, Vander Elst L. Magnetic iron oxide nanoparticles: synthesis, stabilization, vectorization, physicochemical characterizations, and biological applications. Chem Rev. 2008;108(6):2064-110. doi: 10.1021/CR068445E, PMID 18543879.
27. Erkisa M, Ari F, Ulku I, Khodadust R, Yar Y, Yagci Acar H. Etoposide loaded SPION-PNIPAM nanoparticles improve the *in vitro* therapeutic outcome on metastatic prostate cancer cells via enhanced apoptosis. Chem Biodivers. 2020;17(11):e2000607. doi: 10.1002/cbdv.202000607, PMID 32918383.
28. Mandel K, Hutter F, Gellermann C, Sextl G. Synthesis and stabilisation of superparamagnetic iron oxide nanoparticle dispersions. Colloids and Surfaces A: Physicochemical and Engineering Aspects. 2011;390(1-3):173-8. doi: 10.1016/j.colsurfa.2011.09.024.
29. Sun S, Zeng H. Size-controlled synthesis of magnetite nanoparticles. J Am Chem Soc. 2002;124(28):8204-5. doi: 10.1021/JA026501X, PMID 12105897.

30. Lassenberger A, Scheberl A, Stadlbauer A, Stiglbauer A, Helbich T, Reimhult E. Individually stabilized, superparamagnetic nanoparticles with controlled shell and size leading to exceptional stealth properties and high relaxivities. ACS Appl Mater Interfaces. 2017;9(4):3343-53. doi: 10.1021/acsami.6b12932, PMID 28071883.
31. Steitz B, Hofmann H, Kamau SW, Hassa PO, Hottiger MO, von Rechenberg B. Characterization of PEI-coated superparamagnetic iron oxide nanoparticles for transfection: size distribution, colloidal properties and DNA interaction. J Magn Magn Mater. 2007;311(1):300-5. doi: 10.1016/j.jmmm.2006.10.1194.
32. Shen CR, Juang JH, Tsai ZT, Wu ST, Tsai FY, Wang JJ. Preparation, characterization and application of superparamagnetic iron oxide encapsulated with N-[(2-hydroxy-3-trimethylammonium) propyl] chitosan chloride. Carbohydr Polym. 2011;84(2):781-7. doi: 10.1016/j.carbpol.2010.07.067.
33. Baykal A, Amir M, Gunerb S, Sozeri H. Preparation and characterization of SPION functionalized via caffeic acid. J Magn Magn Mater. 2015;395:199-204. doi: 10.1016/j.jmmm.2015.07.095.
34. Graczyk H, Bryan LC, lewinski N, Suarez G, Coullerez G, Bowen P. Physicochemical characterization of nebulized superparamagnetic iron oxide nanoparticles (SPIONs). J Aerosol Med Pulm Drug Deliv. 2015;28(1):43-51. doi: 10.1089/jamp.2013.1117, PMID 24801912.
35. Yu L, Yang X, Wang L, Yang H. Preparation and magnetic properties of doped Ni-Fe/Fe_3O_4 nanocomposite. Materials and Manufacturing Processes. 2011;26(11):1383-7. doi: 10.1080/10426914.2011.577877.
36. Peng N, Wu B, Wang L, He W, Ai Z, Zhang X. High drug loading and pH-responsive targeted nanocarriers from alginate-modified SPIONs for anti-tumor chemotherapy. Biomater Sci. 2016;4(12):1802-13. doi: 10.1039/C6BM00504G, PMID 27792228.
37. Veres P, Sebok D, Dekany I, Gurikov P, Smirnova I, Fábian I. A redox strategy to tailor the release properties of Fe(III)-alginate aerogels for oral drug delivery. Carbohydr Polym. 2018;188:159-67. doi: 10.1016/j.carbpol.2018.01.098, PMID 29525152.
38. Modi S, Anderson BD. Determination of drug release kinetics from nanoparticles: overcoming pitfalls of the dynamic dialysis method. Mol Pharm. 2013;10(8):3076-89. doi: 10.1021/MP400154A, PMID 23758289.
39. Goorani S, Shariatifar N, Seydi N, Zangeneh A, Moradi R, Tari B. The aqueous extract of Allium saralicum R. M. fritsch effectively treat induced anemia: an experimental study on wistar rats. Orient Pharm Exp Med. 2019;19(4):403-13. doi: 10.1007/S13596-019-00361-5.